UNIVERSITY OF CALIFORNIA

SANTA CRUZ

CAUSES AND CONSEQUENCES OF MEANDERING IN BEDROCK RIVERS:

HOW INTERACTIONS BETWEEN ROCK PROPERTIES AND ENVIRONMENTAL CONDITIONS SHAPE LANDSCAPES

A dissertation submitted in partial satisfaction

of the requirements for the degree of

DOCTOR OF PHILOSOPHY

in

EARTH SCIENCE

with an emphasis in GEOLOGY

by

Kerri N. Johnson

March 2016

The Dissertation of Kerri N. Johnson is approved:

_____

Professor Noah J. Finnegan, Chair

_____

Professor Andrew T. Fisher

_____

Dr. Amy E. East

_____

Tyrus Miller

Vice Provost and Dean of Graduate Studies

Table of Contents

Table of Figures

Chapter 1

Chapter 2

Chapter 3

CAUSES AND CONSEQUENCES OF MEANDERING IN BEDROCK RIVERS:

HOW INTERACTIONS BETWEEN ROCK PROPERTIES AND ENVIRONMENTAL CONDITIONS SHAPE LANDSCAPES

Kerri N. Johnson

ABSTRACT

The potential that sinuous bedrock river canyons archive information about past climatic and tectonic forcing of landscapes has intrigued geomorphologists for over 100 years, in fact they were one of the first landforms to inspire the use of landscapes to constrain geologic history. Yet because bedrock river erosion typically requires bedload impacts and abrasion, and because bedload transport is not tightly coupled with the small deviations in fluid shear stress that cause meandering in lowland alluvial rivers, it was never clear how or if the fluid dynamics understood to drive meandering in alluvial rivers could be applied to rivers confined to bedrock canyons. Without a theory for the process of active meandering in bedrock rivers, the assumption that bedrock sinuosity must be inherited from an antecedent alluvial state has remained pervasive despite evidence to the contrary.

In this thesis, exploration of well constrained field examples enables me to formulate two general requirements for a bedrock river to meander: 1. bank-rock must become susceptible to fluid erosion, and 2. mass wasting of steep bedrock cut banks cannot produce persistent talus to protect the bank from continued lateral erosion. With detailed field exploration, experimentation, and mapping, laboratory rock mechanics testing, weathering experiments, topographic analysis and literature

review of mineralogy, we show that where meandering in bedrock occurs, weathering of bank rock satisfies these two conditions. In the mudstone lithology of Pescadero Creek, CA, we show that slaking (fracture due to wetting and drying) of exposed bedrock along cut banks both makes this rock transportable by fluid flow, and makes colluvium easily transportable. For channels in the basaltic lavas of the Kohala Peninsula, Hawai'i chemical weathering can satisfy these same two conditions. This chemical weathering has been shown to be closely controlled by precipitation, and I show a significant decrease in channel sinuosity across the peninsula's strong orographic precipitation gradient from wet to arid regions. In both these examples, meandering is sensitive to climate. This understanding of how bedrock rivers meander provides a mechanistic foundation for climatic interpretations of sinuous bedrock river canyons (including their associated strath terraces).

In addition, I demonstrate that active meandering rearranges drainage networks and has far reaching consequences for landscape evolution and sediment routing. Specifically, I show that 1) growing meander bends can capture tributaries and cause large knickpoints, and 2) meander neck cutoff events cause terraces which isolate adjoining tributaries from the active mainstem, resulting in long lasting tributary convexities, and sediment storage. These autogenic consequences of active meandering mimic tectonic and climatic transience in landscapes over timescales similar to glacial/interglacial cycles (10^5-10^6 years), and also influence sediment transport and storage, which often plays a critical role for aquatic ecosystems.

For Harold Norman Capen

whose infectious love for physics, math, geology, and sharing these with his granddaughter have made my world more exciting and fun

and

For Virginia Winkler Capen

who showed me the joy in words and in solving a good mystery

Thank you to my advisor Noah Finnegan who taught me to look for clever and tractable field problems and to communicate science, to Andy Fisher whose dedication to his students, teaching, and research has set my bar high, and to Amy East for her insightful geomorphic guidance and for reminding me to be proud of this work.

Thank you to the UCSC geomorphology lab, Jon Perkins, Danica Roth, Leslie Hsu, Dave Santaniello, Allison Pfeiffer, Alex Nerson, Claire Masteller, Rachael Klear, and Christian Braudrick, for field and lab help, good discussions, and good times. Thank you to the UCSC E&PS department, especially Priya Ganguli, Nadine Quintana Krupinski, Saffia Hossainzadeh, Rachael Reid, and Naor Movshovitz, and Eli Silver, Gary Glatzmaier, and Matthew Clapham, and to the many undergrads who helped me in the field.

Thank you to Tiffany Liu who learned ArcGIS and Python to make rivers for Kohala and calculate their sinuosity during a high school internship, and Brendan Murphey whose idea sparked Chapter 2.

Thank you to the Santa Barbara City College for giving me a solid foundation in field geology, and to Tony Garcia and Lynn Moody for introducing me to geomorphology and soil science. Thank you to the people of Swanton Pacific Ranch for keeping me

grounded. Thanks to Roberta Smith for her example and for holding me to the highest standards of geology, and to Jim West for reminding me that there are no lines between fields of science, nor art. Thanks to Danica Schaffer Smith, Meg Perry, Leslie Hsu, Megan and Fabian Batista, and Sharifa Crandall for all your encouragement.

Thanks especially to my parents who showed me that no matter where you go there are interesting plants and animals, who have always believed in me, and who taught me that life is more fun when you are learning.

And last, and the opposite of least, Drew Perkins whose enthusiasm for geomorphology reminds me why I love my research at times when none of it is working, checks my spelling, and who has cooked more than his fair share of dinners throughout this process.

The Geomorphology and Land Use Dynamics program of NSF and the Cal State Agricultural Research Initiative provided funding

Thesis Introduction:

Climate and tectonics influence landscapes through their respective influences on erosion. A common goal of geomorphic study is therefore to use landscapes to better understand geologic history and predict landscape response to tectonic and climatic change. Sinuous bedrock rivers were one of the first landforms to spark the study of landscapes as a potential archive of past tectonic and climatic forcing (Davis, 1893; Rich, 1914; Winslow, 1893).

The potential to learn from bedrock river sinuosity is as compelling now as it was in the early days of geomorphology because 1) sinuosity is a sensitive and easily quantifiable landscape metric, 2), bedrock river canyon morphology evolves and persists over much longer timescales than does alluvial river morphology, and 3) actively meandering bedrock rivers are common throughout the world in many lithologies.

Studies of bedrock channel sinuosity over the last 100 years have focused on understanding a variety of aspects of geologic history. In 1893, W. M. Davis first argued that sinuous bedrock rivers were evidence of recent rapid uplift and incision that trapped a previously freely meandering lowland alluvial river within a bedrock canyon (Davis, 1893). Even his contemporaries, however, recognized that topographic features of some bedrock canyons (see chapter 1) require that meandering had been an active process during vertical incision and hence the tectonic interpretation of an uplifted low relief surface is unnecessary (Winslow, 1893). Dury argued that the wavelength of channel bends was set by river discharge and hence

discrepancies between valley shape and the shape of the active channel record shifts in climate (Dury, 1965; Dury, 1972). Unfortunately, the relationship between discharge and the shape of bedrock meanders is still unclear. A notable 2010 study of sinuosity data from bedrock rivers along the western edge of the Pacific Ocean revealed a correlation between sinuosity and both lithology and rainfall variability ("storminess"). After accounting for lithology, these rivers are, on average, more sinuous where precipitation is concentrated into typhoons suggesting that climatic signals may be encoded in these landforms (Barbour, 2008; Stark et al., 2010). The common challenge for these studies is that without a mechanistic understanding of how the development of sinuosity in bedrock river networks occurs, it is difficult to test causal hypotheses.

In contrast to bedrock rivers, the process of meandering in alluvial rivers is easier to observe and has been well studied. It is well recognized that small changes in fluid shear stress induced by a curve in the channel cause outer bank erosion and inner bank deposition (see introduction to Chapter 1). It was not clear however if this understanding of alluvial meandering could be applied to bedrock rivers. The shape and scale of bedrock and alluvial meanders differs (Leopold, Wolman, & Miller, 1964), and it is not intuitive that small changes in fluid shear stress could cause lateral erosion of bedrock at the cut bank. Bedrock river incision generally requires abrasion and impacts from the transport of bedload (Sklar and Dietrich, 2001), but bedload is not necessarily tightly enough coupled with subtle changes in flow to cause meandering. Therefore, without a plausible mechanism, the idea that bedrock river

sinuosity must be inherited from an ancestral alluvial river persists despite ample evidence to the contrary.

This long legacy of interest in bedrock channel sinuosity likely reflects the real potential these landforms have to teach us about external forces that shape landscapes such as climate and tectonics. These interpretations, however, require a fundamental understanding of how the process works, how climate and tectonics interact with this process, and a context for how meandering influences other aspects of landscape evolution.

In this thesis, I use well constrained field examples, detailed field study, rock mechanics tests, weathering experiments, mineralogy literature, and analysis of high resolution topographic data to build this understanding of how a river can actively meander within bedrock banks. I develop and test the hypothesis that physical weathering in mudstone enables erosion by fluid shear stress at cut banks and prevents talus from accumulating and armoring the cut bank (chapter 1). Next, I test if this framework holds in a contrasting lithology (basalt) where chemical, not physical, weathering regulates bedrock strength. A strong relationship between mean annual precipitation and channel sinuosity emerges (chapter 2). Lastly, I use this new foundation of understanding to explore how active bedrock river meandering influence watershed connectivity, erosion patterns, and landscape evolution (Chapter 3).

Chapter 2: Climatic Control on Bedrock Channel Sinuosity: Kohala Peninsula, Hawai'i

Introduction:

The shape of landscapes is controlled, for a large part, by climate and tectonic forcing. A core focus of geomorphology is to develop quantitative ways to extract signals from the topography of landscapes to better understand past climate and tectonics, and to better predict how landscapes may change given future changes to climate and tectonics. In certain rock types, Stark et al. (2010), describe an intriguing pattern between precipitation patterns and bedrock channel sinuosity. In Chapter 1, I argue that physical weathering (via slaking) of exposed rock along bedrock cut banks, in addition to slaking of eroded cut bank colluvium is key to allowing the curvature-induced small changes in fluid shear stress that are known to drive meandering in alluvial rivers (Dietrich et al., 1979; Einstein, 1926; Howard, 1992; Ikeda et al., 1981; Leopold and Wolman, 1960) to result in meandering for rivers confined within bedrock banks. Could other weathering processes besides slaking make cut banks weak enough to be eroded by fluid shear stress, and insure that cut bank colluvium not armor the bank? Most weathering processes are moderated by water and/or temperature and therefore have the potential to be sensitive to climate. Could climate-sensitive weathering moderate the development of sinuosity in some bedrock channels? In this paper, we test the hypothesis that local precipitation influences sinuosity through a control on bank weathering and strength.

Study Site:

To test this hypothesis, we focus on a place where all variables which could influence channel development are fairly uniform, except for climate. The Kohala peninsula, on the Big Island of Hawai'i, is known for one of the world's most dramatic precipitation gradients (Giambelluca et al., 2013) (Fig. 1), and is underlain completely by basalt (Fig. 2). Because of this, the Kohala peninsula has been the site of many studies exploring climatic influences on erosion and weathering (e.g. Chadwick et al., 2003; Goodfellow et al., 2014). Because many channels transverse the climate gradient in different orientations across this landscape, there is the opportunity to explore channel sinuosity given different combinations of upstream flow accumulation and local precipitation.

Bedrock Lithology:

Kohala volcano is the oldest of the 5 shield volcanos that make up the big island of Hawai'i (McDougall and Swanson, 1972). Kohala basalt flows are classified into two groups: 1. The older Pololu Volcanics which makes up most of the volume of the volcano and has a tholeiitic chemistry closer to oxygen-poor mid-ocean ridge basalt; and 2. The Hawi Volcanics which forms a layer on top of some parts of the peninsula is alkalic and has a chemistry and mineralogy closer to a continental basalt (Stearns and Macdonald, 1946) (Fig. 2). The Pololu ranges in age from 260-500ka, and the Hawi flows range in age from 120 - 260 ka (McDougall and Swanson, 1972). The transition to a more continental basalt began in the later Pololu flows, but the Hawi is distinctly more continental than the later Pololu flows (Lanphere and

Frey, 1987). The capping Hawi unit is up to 150 meters thick (Lanphere and Frey, 1987) and made up of a'a flows which are generally 2-5m thick (Spengler and Garcia, 1988). Individual pahoehoe flows of the Pololu are usually less than 1m thick (Spengler and Garcia, 1988).

Climate Gradient:

Northeast trade winds and therefore patterns of orographic precipitation have been consistent over the timescale of the volcano's existence, however the magnitude of rain likely decreases during glacial periods (Chadwick et al., 2003; Hotchkiss et al., 2000; Sanderson, 1993). Due to orographic forcing of precipitation, mean annual precipitation (MAP) increases steadily up the windward northeast side of the peninsula, peaking at over 3m/yr near the drainage divide, and dropping rapidly to less than 30 cm/yr along the south-west coast (Giambelluca et al., 2013)(Fig. 1). Importantly, in the rain shadowed southwest side of the peninsula, some channels begin in areas of high precipitation and travel downstream into areas of very low precipitation, offering the opportunity to investigate channel discharge (as estimated by catchment area and MAP) and local precipitation along a channel where they are not correlated (Fig. 1, Fig. 3).

Climate influence on Weathering of Kohala Peninsula basalt:

Basalt weathering, and therefore basalt strength is generally very dependent on local climate (e.g. Moon and Jayawardane, 2004). Specifically, on the Kohala Peninsula, MAP and its influence on the water balance within a meter of the surface, is a strong predictor of the depth of basalt weathering in both Pololu and Hawi

Volcanics (Hawi: Chadwick et al., 2003; Pololu: Goodfellow et al., 2014). These studies make use of chronosequences on the Kohala Peninsula to describe the relationship between MAP and basalt weathering (including loss of base cations and the depth of weathering profiles). They show that weathering increases non-linearly with increasing MAP until pore spaces are saturated year-round at which point weathering does not increase with increasing MAP.

A'a has a higher porosity and permeability than the more massive pohoehoe flows. This initial basalt flow texture gives a'a more surface area, enables it to collect fine material, hold water, and gives a'a a head start on soil development and weathering over Pohoehoe (Porder et al., 2007). Where a'a and pahoehoe flows are interbedded, the difference in weathering rate is pronounced (Porder et al., 2007).

Lava chemistry is also a fundamental control on chemical weathering rates. In the alkalitic Hawi basalt, iron is more likely to be already bound to oxygen in magnetite crystals, while the relatively oxygen-poor theolitic Pololu basalt has more free iron which may react more easily with water to form hematite (i.e. rust) when exposed at the surface (Spengler and Garcia, 1988). Indeed, red weathering surfaces are common on Pololu flows even in arid areas (Spengler and Garcia, 1988). Both units show a strong correlation between weathering and MAP, but because of these differences I will treat these two lithologies as separate populations in this study.

Murphy et al. (in press) measure the degree of chemical weathering of Hawi basalt located in channel streambeds and find a similar dependence on local

precipitation as Chadwick et. al (2003) found in soils. Murphy et al. demonstrate that climate-dependent chemical weathering physically weakens the bedrock and imparts a strong influence on rates of vertical bedrock fluvial incision.

Study of longitudinal profile slope suggests that fundamental channel-forming processes change across the climate gradient in the same way in Hawi and Pololu basalts (Menking et al., 2013), and models of stream power driven erosion characterize these changes well only when bedrock strength scales with MAP (Han et al., 2014).

Because my previous work (Chapter 1: Johnson and Finnegan, 2015) suggests fluvial bank rock weathering is critical for the development of sinuosity in bedrock channels, here we test the hypothesis that chemical weathering of basalt on the Kohala Peninsula reduces bank strength and reduces the potential for talus and hence enables meandering in the same way physical weathering did in for mudstone in Pescadero Creek. Because it has been shown that weathering is dependent on precipitation and is well described by MAP (Chadwick et al., 2003; Goodfellow et al., 2014; Murphy, in press), we test this hypothesis by comparing the sinuosities of channel reaches across the MAP spectrum from arid (<300mm/yr) to tropical (>2000mm/yr).

Methods:

In order to explore the correlation between sinuosity and factors that might control it, calculations of the sinuosity of channels across the peninsula were needed.

Standard flow accumulation derived channels from the 1/3 arc second DEM (USGSUSGS) were too coarse to capture details of channel planform shape, especially for low relief channels. Therefore, in order to represent channel sinuosity, we used a combination of published hydrology data from the National Hydrography Data Set (USGS) and high resolution USDA orthophotos (USGS, 2012) to digitize bedrock stream paths. From these data we extracted channel sinuosity at points spaced every 10 meters along all channels. Measuring sinuosity requires a simple ratio of the along-path distance of the stream to the straight line distance between two points along it, however it has proven tricky to use this simple metric in comparative studies because the optimal length scale for this measurement may be quite different between or along rivers. To avoid this problem, we measured sinuosity at length scales ranging from 20 meters to 500 meters. We believe this range captures the optimal length scale in most places because sinuosity of individual points along a river typically increased with increasing length scale to some maximum, then decreased at longer length scales. The cases where an optimal was not found and sinuosity gradually increased with length scale overall had very low sinuosities. This method worked quite well where channels had a pattern of regular bends consistent with emergent sinuosity. For these analyses we used the highest sinuosity measured for each point.

Mean annual discharge (m^3/yr) was determined by calculating flow accumulation for each pixel, weighted by MAP. Because precipitation is so far from uniform, weighting this calculation by MAP is essential to accurately predicting mean

annual discharges accurately. Because the low relief dry side channels are not well-expressed in the DEM, they were not accurately extracted from the DEM using a flow accumulation algorithm. Consequently, as mentioned above, we used orthophotos to accurately define channel planform shapes on the dry side. Because of this approach to digitization of channels, however, the points for channels don't necessarily fall within areas of high flow accumulation. This problem can be overcome, however, by locating the highest flowing accumulation value in a radius around each channel point. For the analysis here, a radius of 60 meters was used, and the results were vetted for artifacts of the coarse DEM.

Channels were clipped at a discharge equivalent to the debris flow-fluvial slope area scaling break observed by Stock and Dietrich (2003), at catchment areas of $\sim 10^5\ m^2$. Because precipitation is so far from uniform across the study area, we started channels on the landscape at a discharge of $10^5\ m^3/yr$, equivalent to this scaling break with MAP of 1m/yr which is on the order of MAP for the channels observed by Stock and Dietrich (2003). These estimations neglect the influence of infiltration, groundwater flow to streams, and evapotranspiration. These assumptions are addressed in the discussion.

In addition to MAP and metrics calculated from the DEM such as elevation and slope, geospatial data for basalt flow unit and flow age came from USGS mapping (Wolfe, 1996).

Field observations were made in two channels on the dry side where local precipitation and flow accumulation gradients are inversely related. These include Schmidt Hammer measurements of rock strength and surveys of the channel thalweg, cross-section, and alluvial cover. Bedrock strength measurements were made using a Type-N Schmidt hammer at equal intervals along stream parallel transects in the streambed. Although this tool directly measures in-situ rock elastic properties, the values have been shown to linearly scale with tensile strength of the rock, which is important given rocks fail in tension when subjected to low-velocity particle impacts (Johnson, 1972).

Resul**ts:**

Qualitatively, channel sinuosity is generally higher on the wetter northeast side of the island, especially in downstream reaches of the older Pololu basalt (Fig. 1, 2). Whether channels tap into even wetter headwater regions to the west doesn't seem to have as much of an influence on the sinuosity of northeast wet side channels as the basalt unit does (Fig.1, 2).

In the rain shadow on the southwest side of the peninsula, channels in both flow units generally have much lower sinuosities (Fig. 2,4). However, on the southern part of the southwest "dry side" of the peninsula, some channels begin in areas of higher MAP (Fig.2, 3). These dry side channels provide a unique opportunity to explore the variables of local MAP (local climate) and accumulation of upstream flow (mean annual stream discharge) because these channels flow down a

precipitation gradient of almost an order of magnitude, from over 2000 mm/yr at their headwaters, to less than 300 mm/yr at the sea. These channels are more sinuous at their headwaters than downstream, the opposite of the wet side channels. The contrast is visually striking and channels quickly straighten out when they leave areas of high local precipitation (Fig.1, 3, 5).

Two primary variables that influence active bedrock meandering, and which are influenced by climate, are the channel discharge, which integrates upstream precipitation within the catchment area for a channel reach, and bank strength and bedrock weathering which are functions of local precipitation. The distribution of sinuosity shows a strong pattern of higher sinuosities at higher MAP values (Fig. 6a). This pattern is not gradual but shows a pronounced transition to higher sinuosities at around 1200 mm/yr local precipitation (Fig. 6a). Surprisingly, high sinuosities are distributed across the full range of mean annual discharge values (Fig.6b).

In the rain shadow on the SW side of the peninsula, we explore discharge further. We utilize the fact that local precipitation trends in the opposite direction of discharge (high MAP at low discharge headwaters, low MAP at higher discharges downstream) to explore the influences of local climate and discharge separately. Figure 3 shows qualitatively that sinuous channels straighten out quickly as they cross into drier areas downstream. A closer look at an example, Kawaihae Gulch (indicated on Fig. 1 and 3), shows that as MAP decreases downstream, MAD increases (Fig. 5). Slope of the channel is quite consistent. Sinuosity starts low,

begins to increase after about $1x10^6$ m^3/yr discharge and becomes low again once MAP drops below about 1750 mm/yr.

Besides MAP and mean annual discharge, we explored other variables that might be expected to influence channel sinuosity such as slope, channel relief (i.e. incision into the initial volcano surface), and basalt flow unit (Pololu or Hawi). Local MAP has the strongest influence on sinuosity, however, basalt flow unit also clearly has a large influence on sinuosity (Fig. 4). Both Hawi and Pololu basalts have similar distributions of low sinuosity rivers where MAP is less than 1400 mm/yr (Fig. 4). In areas with higher MAP, however, the younger Hawi basalt flows (120 - 260 ka) support more sinuous rivers than dry areas, but older Pololu flows (260-500 ka) support the most sinuous rivers (Fig. 4). Figure 4 is shown with the data separated by water balance zones (as estimated by MAP) for the Hawi (Chadwick et al., 2003), this is may be a conservative estimate however for the Pololu which reaches year-round saturation at lower MAP (Goodfellow et al., 2014).

A key observation from the field is that bedrock exposed in the thalweg of the channel decreases with increasing local MAP, consistent with findings in other Kohala channels (Murphy et al. in press). In addition to rock strength decreasing with local MAP in the thalweg, bedrock strength also decreases with height above the thalweg. This finding is consistent with previous work showing spatial variations in rock strength with height in channel cross-sections (Small et al., 2015). However, our results additionally demonstrate that this loss of strength up the bank is increasingly pronounced with increasing local mean annual precipitation. In the region with the

highest sinuosity (Fig. 2, 3, 5), streambeds are still competent bedrock, while the banks have weathered to saprolite such that they can easily be scooped out with your hand. Additionally, in this same region of high sinuosity, depositional point bars were observed paired with clean swept bedrock cut-banks. These features which are important for meandering were not observed in other parts of the channel.

Discussion:

Clear climatic control on sinuosity:

On the Kohala peninsula, we observe a strong pattern in channel sinuosity across a pronounced rainfall gradient, with higher sinuosities found in areas of high local MAP above about 1100mm/yr (Fig. 6a). Strikingly, no significant trend was observed between sinuosity and mean annual discharge.

Channels cutting through Pololu Volcanics had a stronger trend towards more sinuous channels with MAP above 1400mm/yr than did channels in the Hawi Basalt, though both had similarly straight channels below 500mm/yr. It is not clear from this analysis if this is because the Pololu Volcanics are twice as old (260-500 ka as opposed to 120-260 ka age of Hawi Volcanics) and have therefore been exposed to a wet climate for longer, or if weathering rates in the two basalt units have different rates or styles of weathering. Despite these differences, data from both units strongly suggest that exposure to a climate conducive to chemical weathering is the primary controls on the sinuosity of channels on the Kohala Peninsula.

This supports our model for the development of sinuosity in bedrock channels developed in Chapter 1. There, our analysis pointed to rock strength and bedrock

weathering potential as key to active bedrock channel meandering (Chapter 1: Johnson and Finnegan, 2015). In that chapter we showed that if bedrock is made erodible by fluid flow, and if colluvium from steepened cut banks does not armor the bank and act as a strong negative feedback on further lateral fluid erosion, then a bedrock channel can meander in the same manner as an alluvial river and higher channel sinuosities can develop within bedrock banks (Chapter 1: Johnson and Finnegan, 2015).

Areas for further investigation:

Our calculated discharge doesn't take into consideration infiltration or evapotranspiration. Further investigation is warranted to test how representative our estimations of channel flow actually are. On the dry southwest side of the peninsula, most channels are intermittent with the notable exception of some of the channels that tap into zones of high precipitation in their headwaters such as Kawaihae Gulch (Fig. 5). Intermittent streams commonly lose flow to groundwater along their path so the fact that channels with high precipitation at their headwaters consistently transmit flow across the arid lava to the sea (Murphy and Finnegan personal communications) suggests that infiltration doesn't completely invalidate our discharge estimations. Unfortunately none of these channels have available gauge data. Measuring discharge along these channels would be an illuminating next step.

In this study, I have considered MAP, and mean annual discharge. For the consistent trade wind dominated orographic precipitation, this is likely an acceptable way to explore representative conditions. On the wet northeast side of the peninsula,

this orographic precipitation is a dominant source of channel discharge, and although larger storms do also occur, this is likely a good way of exploring channel forming flows. For dry side channels however, occasional "Kona" storms from the south likely are a dominant source of precipitation. These storms have a longer recurrence interval and may not be captured in annual data; therefore, for the dry side, mean annual values for precipitation and discharge may grossly underestimate the volume of the dominant "channel forming" discharges. Further investigation into the temporal distribution of precipitation is likely needed to gain a better idea of the relationship between channel discharge and the planform shape of channels here.

Conclusion:

On Kohala Peninsula, sinuosity correlates strongly with local precipitation. These results, in combination with past studies on Kohala basalts, suggest that local precipitation-driven chemical weathering is what ultimately drives the development of sinuosity in bedrock channels. While other factors may influence the ability to develop the flow patterns required for meandering to drive lateral erosion of cut banks, rock strength and its erodibility is the first-order control on where the development of sinuosity is possible. This mechanistic model of weathering driving the development of sinuosity in bedrock channels is consistent with previous work looking at cross-sectional distributions of bedrock strength, weathering and river erosion (Hancock et al., 2011; Montgomery, 2004; Small et al., 2015), and meets the conditions for meandering set forth in Chapter 1 (Johnson and Finnegan, 2015). This

provides a first mechanistically-based model for the relationship between climate and the development of bedrock river sinuosity.

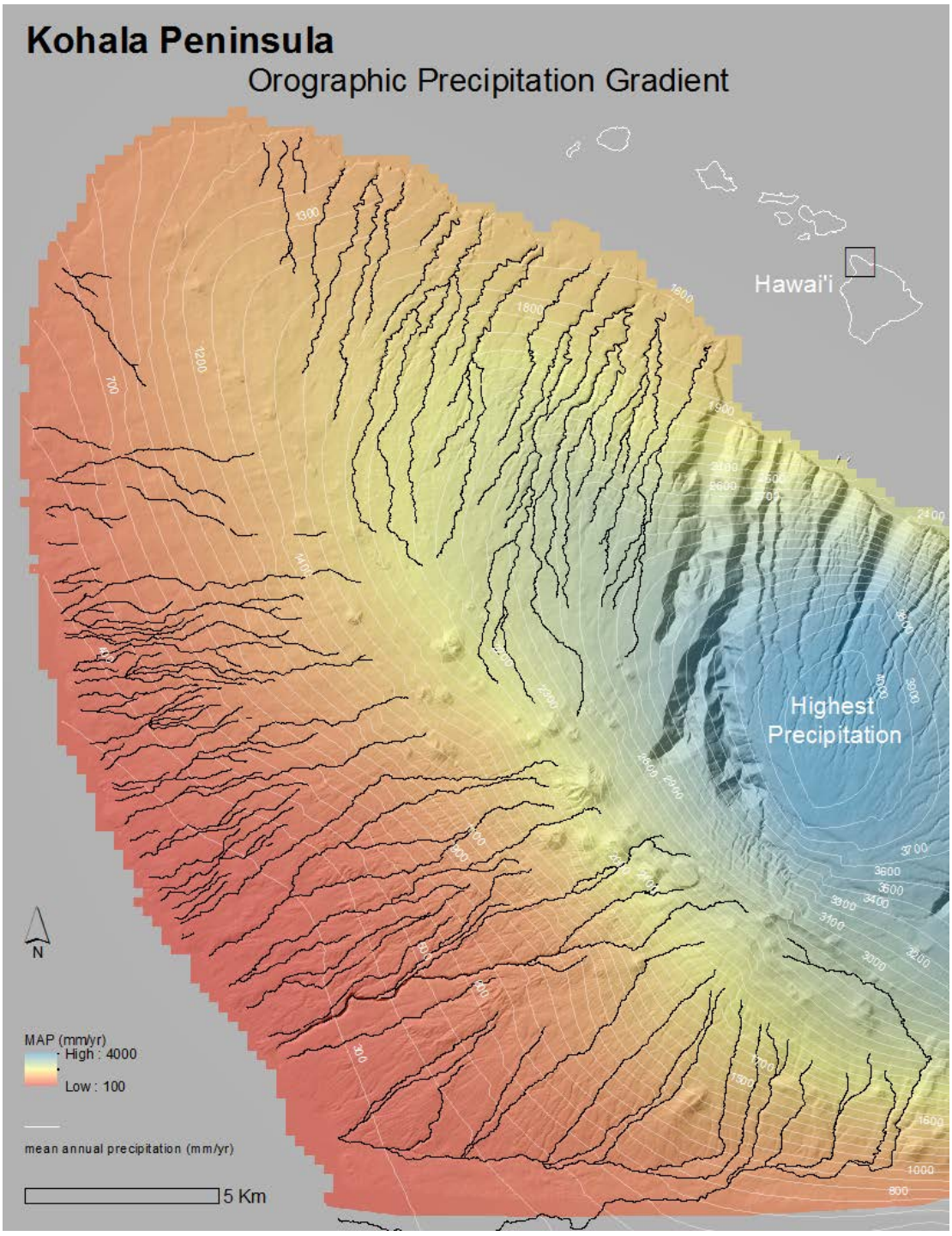

Figure 1. Orographic precipitation from consistent trade wind moisture causes high precipitation on the northeast side of the Kohala Peninsula and an arid rain shadow on the southwest side.

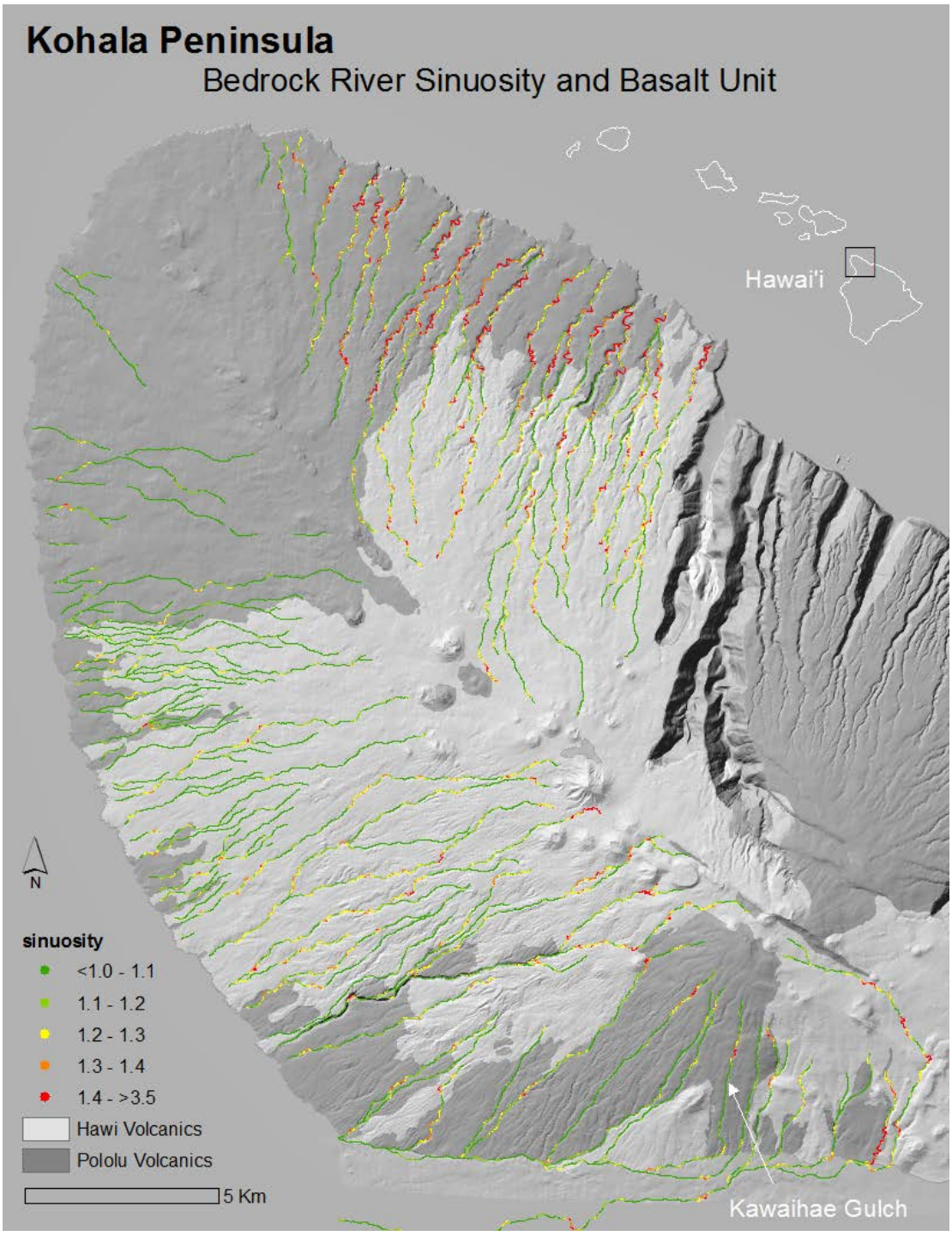

Figure 2. Kohala Volcano is the oldest part of the big island of Hawai'i. Pololu Volcanics make up most of the volume of the island with Hawi Volcanics blanketing some of the Peninsula. Data from Kawaihae Gulch is presented in Fig. 5.

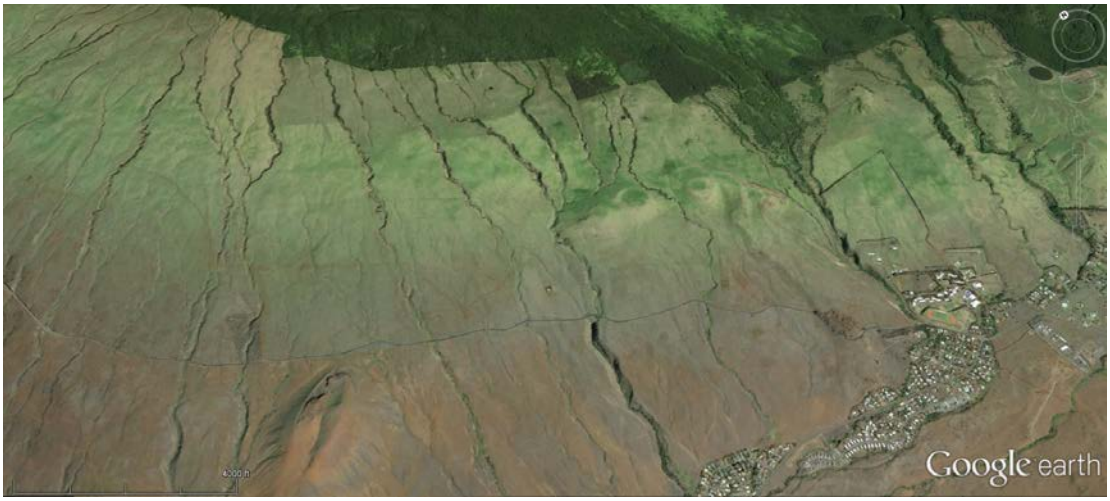

Figure 3. The dry southwest flank of the peninsula has high MAP at higher elevations and low MAP downstream near the coast. Channel sinuosity is generally higher upstream in the wetter climate zone. This rain shadow provides a great opportunity to deconvolve local precipitation and flow accumulation.

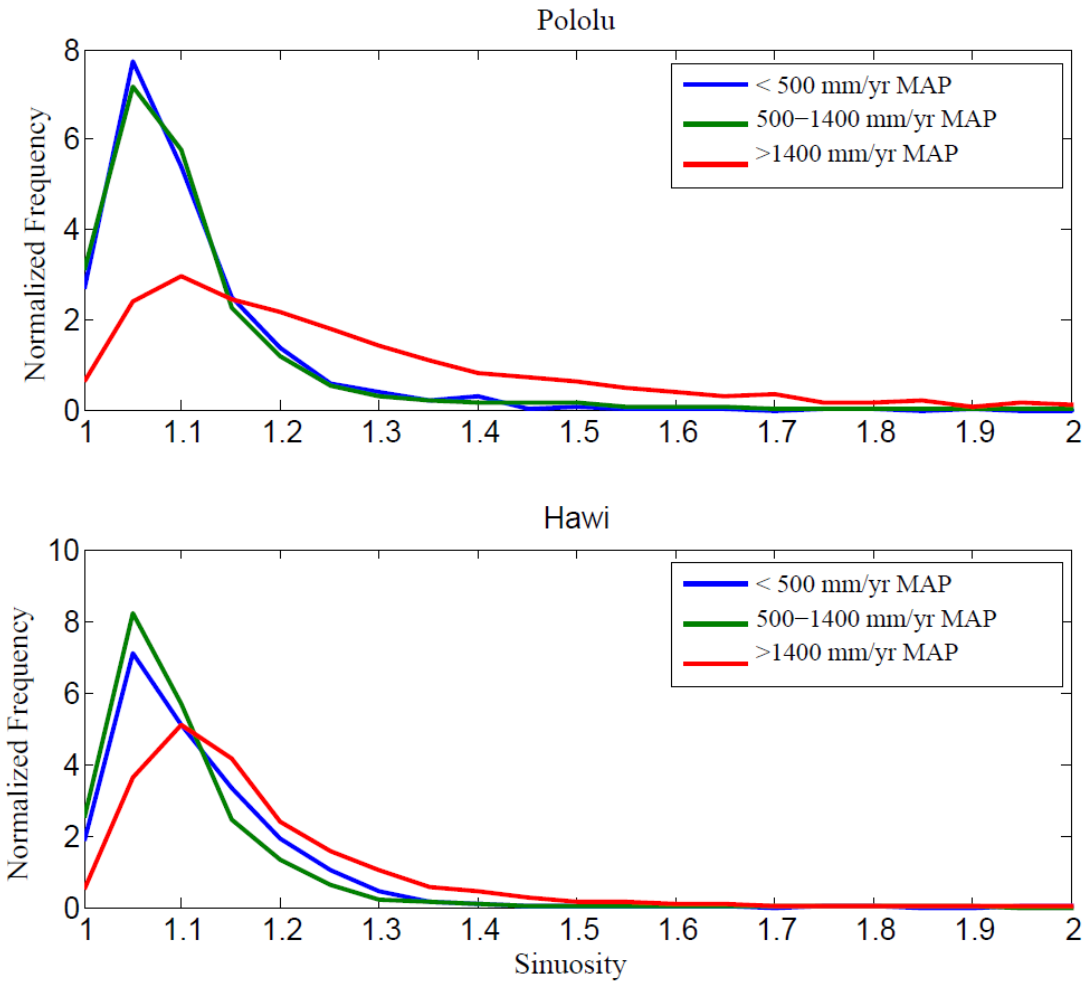

Figure 4. Sinuosity data is grouped by the functional MAP zones for weathering outlined in Chadwick et al. (2003). Locations on the peninsula with <500 mm/yr MAP have year a round negative water balance and very little chemical erosion, >1400 mm/yr MAP have a year round positive water balance and deep erosion. The zone in-between sees seasonal shifts. Sinuosity distributions are similar for all except the >1400mm/yr group in both basalt units. The Pololu >1400mm/yr group is shifted farther towards sinuous then the Hawi group for the same MAP.

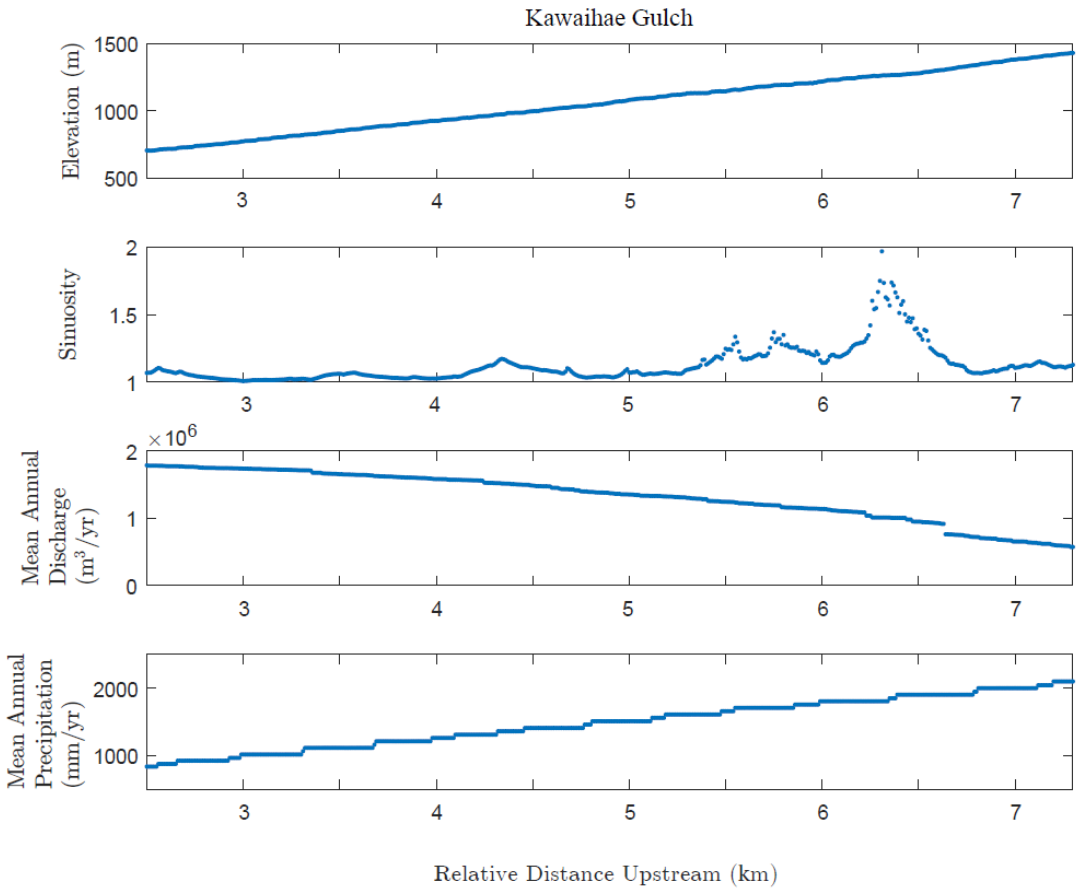

Figure 5 As Kawaihae Gluch begins its path down towards the arid southwest side of Kohala Peninsula, its sinuosity increases up to a point then rapidly decreases again. When accumulated discharge and local MAP both increase downstream sinuosities stay high, supporting the hypothesis that less weathered bedrock at low MAP is preventing the development of sinuosity.

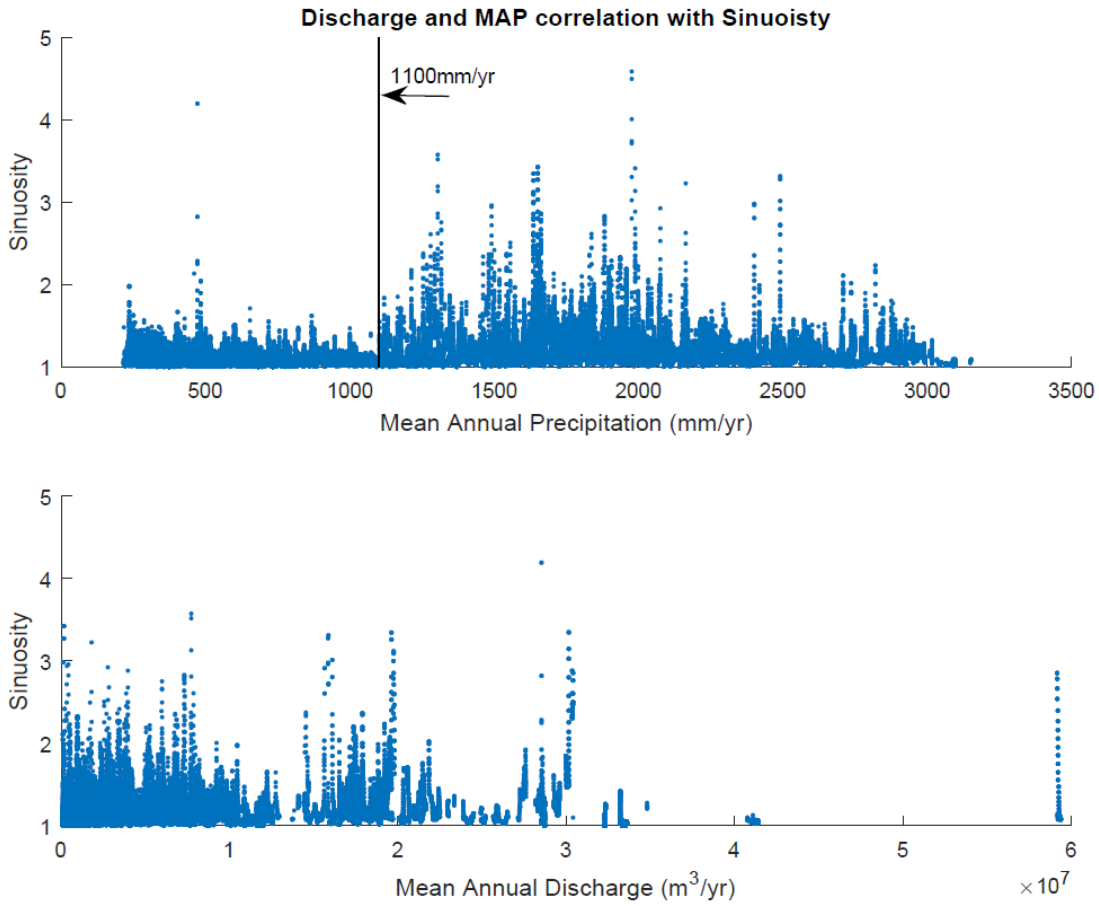

Figure 6. Sinuosity data show an abrupt increase at about the 1100mm/yr threshold for weathering of Pololu Basalt found by Goodfellow et al. (2014). No such trend is seen between mean annual discharge and sinuosity.

Chapter 3: Autogenic Drainage Network Reorganization from Bedrock River Meandering in the Oregon Coast Range, USA

Abstract:

Bedrock rivers set the pace of erosion across most landscapes. Therefore analysis of these river networks is the most common and direct way to study the balance between mountain building and erosion (Whipple, 2004; Wobus et al., 2006). Deviations away from constant erosive potential across landscapes are often interpreted to reflect transience resulting from shifts in climate or variations in tectonic uplift (e.g. Schoenbohm et al., 2004). Such a perspective, however, relies on the assumption that the planform shape of rivers is fixed in space and time (Howard et al., 1994). Here, via analysis of high-resolution topographic data, we show that the meandering of a mainstem channel in the Oregon Coast Range (USA) triggers large-scale autogenic variation in tributary long profile slopes and drainage network architecture in two fundamental ways. First, capture of tributary long profiles by the meandering mainstem channel steepens the captured tributaries and localizes tributary confluences to the apex of growing bends. Second, mainstem meander cutoffs isolate connecting tributaries from the effects of the relative base-level fall of the mainstem, leading to hanging tributary valleys that persist over 10^5-10^6 year time scales. We show that meandering-driven bedrock drainage reorganization imparts transient bedrock river slope-area signals which mimic signals related to climatic or tectonic fluctuations, and which prevent the landscape from achieving a topographic steady state.

Introduction:

Bedrock river channel slope is argued to record a competition between tectonic uplift (which influences relative base-level) and climate (which influences river discharge) (e.g. Leopold and Bull, 1979; Snyder et al., 2000; Whipple, 2004). The erosive potential of a bedrock river is a function of its slope and accumulated drainage (e.g. Howard and Kerby, 1983). Given constant rates of tectonic and climatic forcing, slope is thought to evolve until erosion rates match uplift rates uniformly across a landscape, creating an equilibrium or steady-state landscape (Snyder et al., 2000). For this reason, the topography of bedrock river channels is a common focus of tectonic geomorphology studies. In general, the framework that has been developed for analyzing river profiles assumes a fixed bedrock channel network (e.g. Wobus et al., 2006) and typically ignores the possibility of autogenic fluctuations in channel slope and erosion rate, although such autogenic fluctuations are observed in physical experiments along with lateral channel mobility (Hasbargen and Paola, 2000). In bedrock channels, meandering is the most common mechanism for lateral channel motion and active bedrock river meandering is ubiquitous in settings where bedrock rivers shape landscapes, particularly in sedimentary rocks that fringe many active mountain belts (e.g. Finnegan and Dietrich, 2011; Lavé and Avouac, 2000; Shyu et al., 2006; Stark et al., 2010). Here we provide evidence and a conceptual model showing that bedrock meandering can trigger large-scale autogenic fluctuations. We focus on the Oregon Coast Range (OCR) because it is considered an archetypal steady state landscape due to its generally uniform lithology, vegetation,

climatic past (no recent glaciations) and its constant rates of rock uplift over time (Heimsath et al., 2001; Kobor and Roering, 2004; Personius et al., 1993; Reneau and Dietrich, 1991).

Like most major rivers in the OCR, the river we examine here, the Smith River, is actively meandering within bedrock banks (Fig. 1) (Personius, 1995). Examples from the Smith, described below, show that the lateral drainage mobility inherent to meandering not only moderates vertical incision by creating neck cutoff knickpoints on the mainstem (Finnegan and Dietrich, 2011), but that interactions between tributary channels and a meandering mainstem channel cause frequent reorganizations of the drainage network connectivity and introduce large-scale autogenic fluctuations in channel slope and erosion rate. From these examples, we build a conceptual model for watershed-scale disequilibrium that should be expected in watersheds where bedrock rivers are laterally mobile.

Methods:

Data sources:

Three foot gridded bare earth LIDAR data for the Smith River (flown in 2008) were acquired from the Oregon Department of Geology and Mineral Industries (DOGAMI). The area within this dataset that was considered in this study is the Smith River watershed from the eastern upstream extent of the Twin Sisters Quadrangle (extent of the LiDAR we had), downstream to just above reaches which may be influenced by a backwater effect. When parts of the watershed were not

covered by LiDAR data, flow accumulation was passed into the study area from the 1/9 and 1/3 arc second USGS National Elevation Dataset data.

Definition of tributary channels:

Channels were extracted from the LiDAR data via routing of accumulated flow. Pixels with catchment area over 1.5 km^2 were considered channels. All tributaries within the study area that met this definition of channels were considered in this study.

Cutoff analysis:

Cutoff terraces were considered only where clearly identifiable in the LiDAR data by a central hill surrounded by a low relief surface that trended away from, then back to the modern Smith River (Fig. 2a). More cutoffs were identified than were used in these analyses because we only considered the most certain examples. Careful examination of these terrace surface using x-sectional profiles, fine topo lines, and breaks in slope were used to piece together the original surface elevation of the original cutoff mainstem reach where incision into or deposition onto the original surface has likely occurred. Only examples where this could be inferred were used. Because these terrace surfaces were sloped, we estimated the downstream terrace elevation (often lost to incision) from the best preserved location on the terrace surface using the distance along the bend and assuming the average modern mainstem slope. Measurements of mainstem incision below the meander cutoff were calculated

by subtracting the modern mainstem Smith River elevation at the cutoff from this downstream terrace elevation. We estimate the time since the cutoff occurred using this incision distance and the steady long term vertical incision rate for the Smith River (Personius, 1995) (Fig.2b).

χ-profiles

We decided to use χ analysis (Perron and Royden, 2013) to study these long profiles because this method accounts for the influence of flow accumulation on channel slope. Therefore, the concavity due to downstream accumulation of flow, and slope changes at tributary junctions that are common in long profiles are removed. This leaves a profile with a slope that can be thought of as the channel's erosive potential (a function of channel slope and flow accumulation). Channel reaches with steeper slopes in χ-space can be expected to have more erosive potential, and therefore faster incision into bedrock than channel reaches with shallower slopes (Perron and Royden, 2013; Willett et al., 2014). Therefore, if bedrock strength, and other factors that determine how much erosive potential is needed for a certain vertical channel incision rate, are assumed constant along a profile that is fully adjusted to a steady background uplift rate, the slope in χ-space will be constant. The Smith River, in the Oregon Coast Range was chosen as a study site because its consistent lithology, vegetation, and reputation as a "text book" steady state landscape, make it one of the few places where channels can be assumed to be adjusted to long term steady uplift rates, thus having linear profiles in χ-space. Our

analysis of tributary χ-profiles in this study looks for predictable deviations away from "steady state" due to meander-driven cutoff and capture.

To create these profiles, distance along tributaries, elevation, and flow accumulation data was taken for points every 10m from the DEM (see above) and χ was calculated (per Perron and Royden, 2013) using a reference concavity of .5.

In order to estimate the timescale it takes for a tributary to recover to a linear steady state profile after cutoff, we assumed the original tributary portion of the profile was in steady state before the cutoff, and the slope of these linear profiles represented "steady state". We projected that straight line profile through the newly appended terrace (former mainstem) to estimate the amount of modern mainstem incision necessary before there is enough relief for the profile to reassume the original steady state χ profile slope all along the tributary profile (Fig. 2b). Using the Personius (1995) estimation of the rate of mainstem incision we convert this required incision to a time to recovery (Fig. 2b). This is a conservative estimate of recovery time, because many profiles with sufficient mainstem incision still have large convexities through this terrace region and are not yet linear as is expected once they reassume steady state. For these profiles, we estimated the amount of modern mainstem incision past what is needed for a linear profile. Because these profiles are still out of equilibrium, these distances, converted to time, give a sense for how long these profiles have been transient, and how much we underestimate actual times to re-equilibrium by using previously described method.

Captures:

At each tributary confluence, the radius of curvature of the mainstem Smith River was calculated by fitting a circle to points every 10 meters along the river for 50 meters up and downstream of the confluence using a least squares best fit. These radius of curvature data were separated into two groups based on whether the tributary joins the river from within the circle (joining along a convex bank, from the point bar) or joining from the outside (joining along a concave bank, from the cut bank). All tributaries within our study area meeting the drainage area threshold discussed above were included.

Results:

Mainstem neck cutoffs isolate tributaries from base level lowering:

Actively meandering bedrock rivers often produce neck cutoffs (e.g. Finnegan and Dietrich, 2011). Given steady state conditions, before cutoff, tributary and mainstem channel slopes should be adjusted to incise at the steady state landscape lowering rate. Tributaries are steeper than the mainstem at steady state due to their smaller catchment areas. After a low-slope mainstem reach becomes a neck cutoff terrace and loses the mainstem's flow, adjoining tributaries must cross it with only the tributary drainage to reach the new mainstem location (Fig. 2a). Therefore, this segment is left with tributary-scale flow, but mainstem adjusted slope, and has much lower erosive potential than needed to keep pace with the incision rate of the mainstem (Leopold and Bull, 1979).

A steady state profile in χ-space should be linear because its slope is adjusted for drainage area everywhere such that incision rate can match a steady uplift rate all along the profile (assuming constant rock strength, precipitation rates, erosion mechanisms, etc. along the profile) (Willett et al., 2014). In contrast to linear steady state profiles, in Smith River examples we observe tributary profiles with steep upper reaches and low slope reaches where the channel flows across the cutoff mainstem meander bend terrace (Fig. 3). Aggradation is often observed where the steep original tributary joins the low slope appended paleo mainstem reach (Fig.3, 2b, 4). In addition, at these locations there is typically an extremely steep reach at the downstream end of the cutoff terrace where the tributary joins the active mainstem. This steep reach records the differential incision following the meander cutoff between the mainstem and the stranded tributary reach (Fig. 2b, 3-5). The Smith River examples vary in the amount of upstream propagation of this steep segment, and hence the amount of progress towards reduction of the convexity and the attainment of a new steady-state profile (Fig. 3, 5-4).

We report measurements of mainstem incision below the meander cutoff elevations as an estimate of the time since meander bend cutoff (methods). We use estimates of river incision rates within rivers of the central Oregon Coast Range, and specifically the Smith River (Personius, 1995) in order to convert the magnitude of incision below meander cutoffs into a time-scale since abandonment of the cutoff. If tributaries preserve large convexities and therefore not yet re-established linear steady state profiles (Fig. 2b, 3-5). By projecting the steady-state slope from the original

linear tributary segment to the new confluence we estimate minimum times for re-equilibration of these tributaries (Table 1, Fig.2b), which again is a minimum estimate of transience as our examples show profiles at this stage still exhibit large convexities (Fig.3-5). According to these conservative topographic estimates, after mainstem cutoff, tributary transience persists on the order of at least 10^5-10^6 years (Table 1). While this convexity persists, the watershed upstream is isolated from external base-level fall until the convexity is removed from the profile (Leopold and Bull, 1979). Cutoff terrace surfaces are likely eroded before the influence of these events is lost from tributary long profiles, and here (Fig. 1, 3-6, Table 1) we only include young examples with clear terrace surfaces remaining, therefore likely underestimating transience time scales following cutoff events.

Capture of tributaries by a meandering mainstem:

If a propagating mainstem bend meanders into a tributary channel, it will typically provide a steeper, more efficient path for that tributary, and result in a capture event (Fig. 7). Figure 8a shows an example of a mainstem meander bend that is growing toward a tributary channel as is clear from the strath terraces on the inside of the bend, and the striking asymmetry at the bend apex, (Johnson and Finnegan, 2015).

In χ-space (Fig. 8b), the profile of the tributary currently (blue solid) has a relatively uniform slope along the profile (methods), suggesting that incision is likely in steady-state, thereby keeping pace with the rate of relative base level lowering induced by tectonic uplift. Once this tributary is captured, the portion of the tributary above the capture point will have a steep knickpoint, in this case, the elevation

difference between the tributary and the mainstem reach that is about to capture it is ~ 70 meters. In χ-space this segment is very steep with high erosive potential after capture. Accordingly, the section of the tributary below the imminent capture point will lose some of its drainage area. This segment (Fig. 8b blue-dashed) will then lose erosive potential due to the loss of catchment area, and will likely be unable to incise at the pace of uplift, thereby growing/preserving a localized low-relief surface (e.g. Yang et al., 2015).

If this capture of tributaries by meander bends is relatively common in a landscape, then the signature of this process should be visible in the drainage network. Figure 9 shows curvature data from the mainstem river at the confluence of each tributary (methods). These data show that tributaries are not distributed uniformly along the mainstem channel, but instead cluster along the high curvature leading edge of propagating meander bends. In our example (Fig. 8a), the pre-capture tributary joins the Smith River along a low-curvature reach, however after the capture event, the upstream portion of the tributary will have its new confluence with the mainstem at the highest curvature leading edge of that migrating bend, the most commonly observed location for tributary confluences in the Smith River network (e.g., Fig.9). Tributaries joining at the leading edge of meander bends are more common than would be expected for random points (hypothetical confluences) placed along the Smith river mainstem (above the 95% confidence interval).

Discussion:

Our results show that bedrock river meandering is an autogenic driver of landscape disequilibrium at the sub-watershed scale in a landscape that is commonly argued to reflect steady tectonic and climatic forcing. Because internally generated signals mimic the landscape response to changes in climate, tectonics or base level forcing, this poses a challenge to the interpretation of landscapes solely in terms of these external drivers. Specifically, we show that channel steepness (when normalized for drainage area) can vary by an order of magnitude among the numerous tributaries affected by cutoffs and by captures (Fig. 3, 8b, 4, 5). Hence, propagating base-level signals related to changes in rates of tectonic uplift would be superimposed on these large autogenic channel steepness signals in tributaries, making it challenging to disentangle internally and externally generated river slope signals. In addition, our results provide evidence that timescales of transience in tributaries affected by meandering are comparable to or in excess of the timescales of Pleistocene forcing of climate and sea-level. Therefore, from the perspective of interpreting climatic forcing of landscape evolution, it is unlikely that climate signals could be easily recovered from tributary long profile data.

Conclusion:

Because these mechanisms for slowing and accelerating base-level lowering rates operate at the tributary watershed scale, adjacent sub-watersheds can be expected to have very different erosion rates. These differences in erosive potential across drainage divides should lead to divide migration (Willett et al., 2014) and

further changes in tributary drainage patterns, thereby introducing a third source of autogenic transience in landscapes with actively meandering bedrock rivers. These three internal processes not only mask signals of external landscape forcing, but they may prevent landscapes from ever achieving a spatially uniform steady-state form. Finally, the processes of capture and cutoff lead to reorganization of drainage network connectivity on a time scale that is comparable to the growth of meander bends. Changing the routing of flow across a landscape has implications for ecosystem and species connectivity, surface and groundwater hydrology, and the storage and transport of sediment.

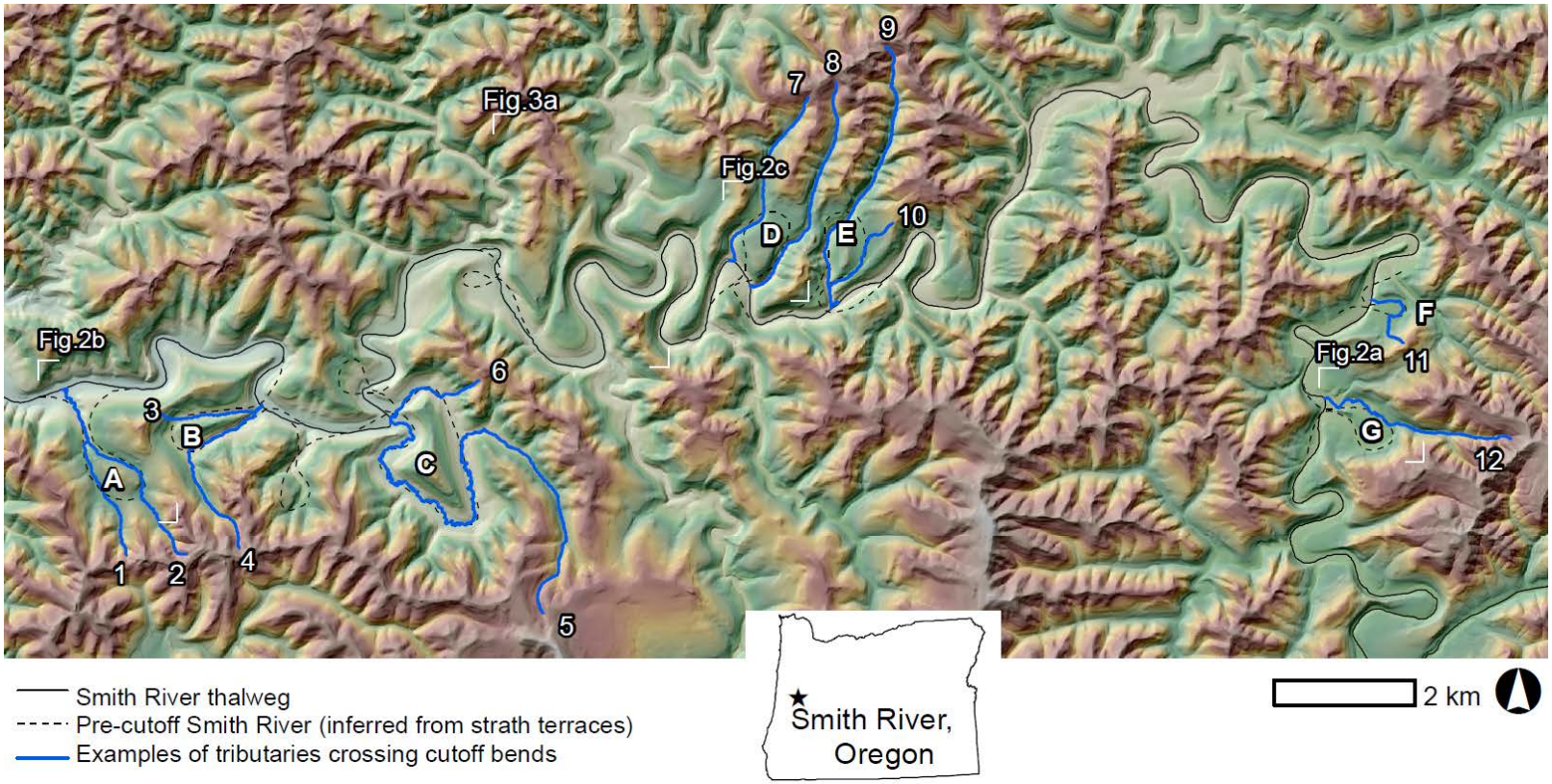

Figure 1. The Smith River, in the Oregon Coast Range, displays all the signs of active meandering including neck cutoff terraces (clearest examples labeled A-G with adjoining tributaries labeled 1-12).

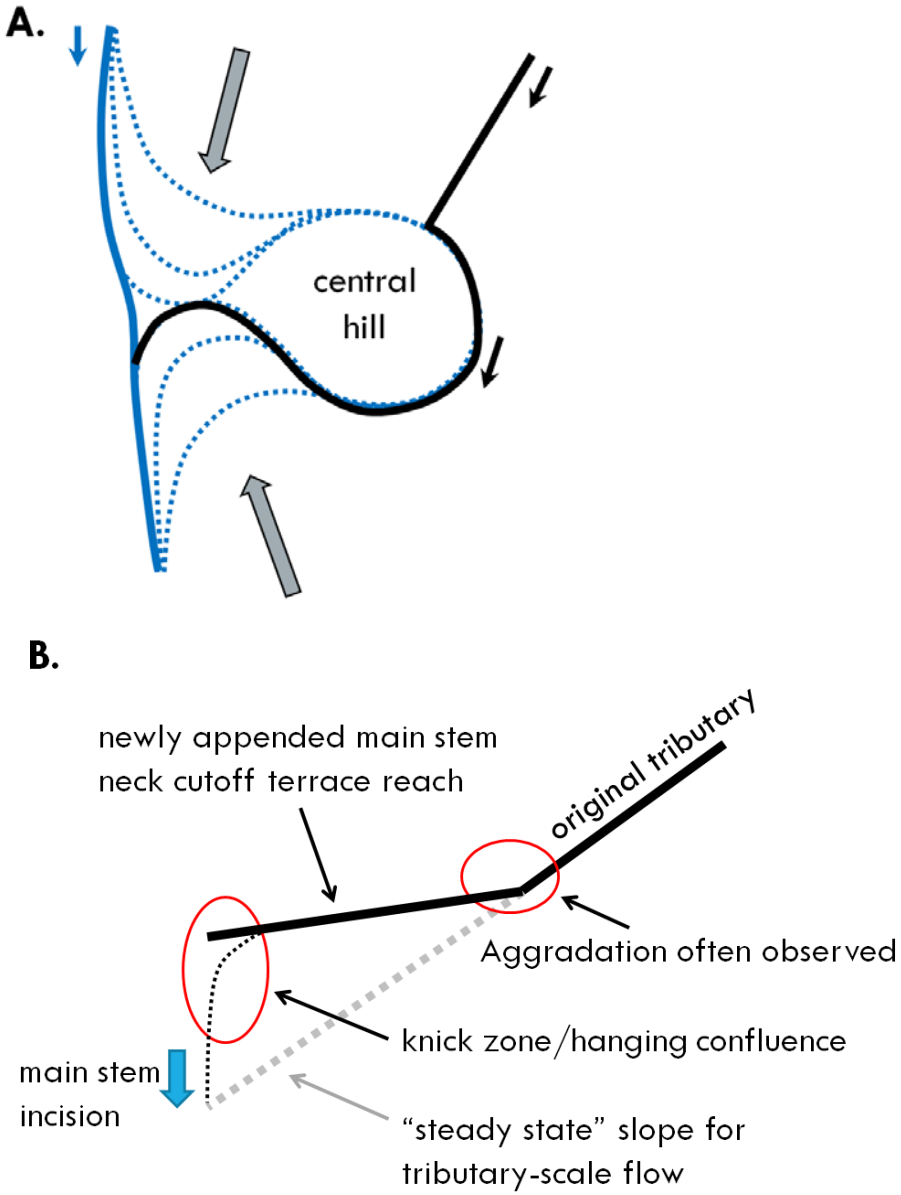

Figure 2 a. Tributary adjoining cutoff meander bend must cross terrace to reach modern main stem. **b.** Low gradient main stem terrace is appended to lower reach of tributary profile. Projecting the original profile down in χ space is an estimate of how much main stem incision (blue arrow) is necessary before re-equilibration is possible. Timescales of transience can be estimated given constant background incision of .1 to .3mm/yr (Personius, 1995). This is a conservative estimate because many modern

profiles have had enough main stem incision, or have overshot that, but still exhibit transient profile convexity

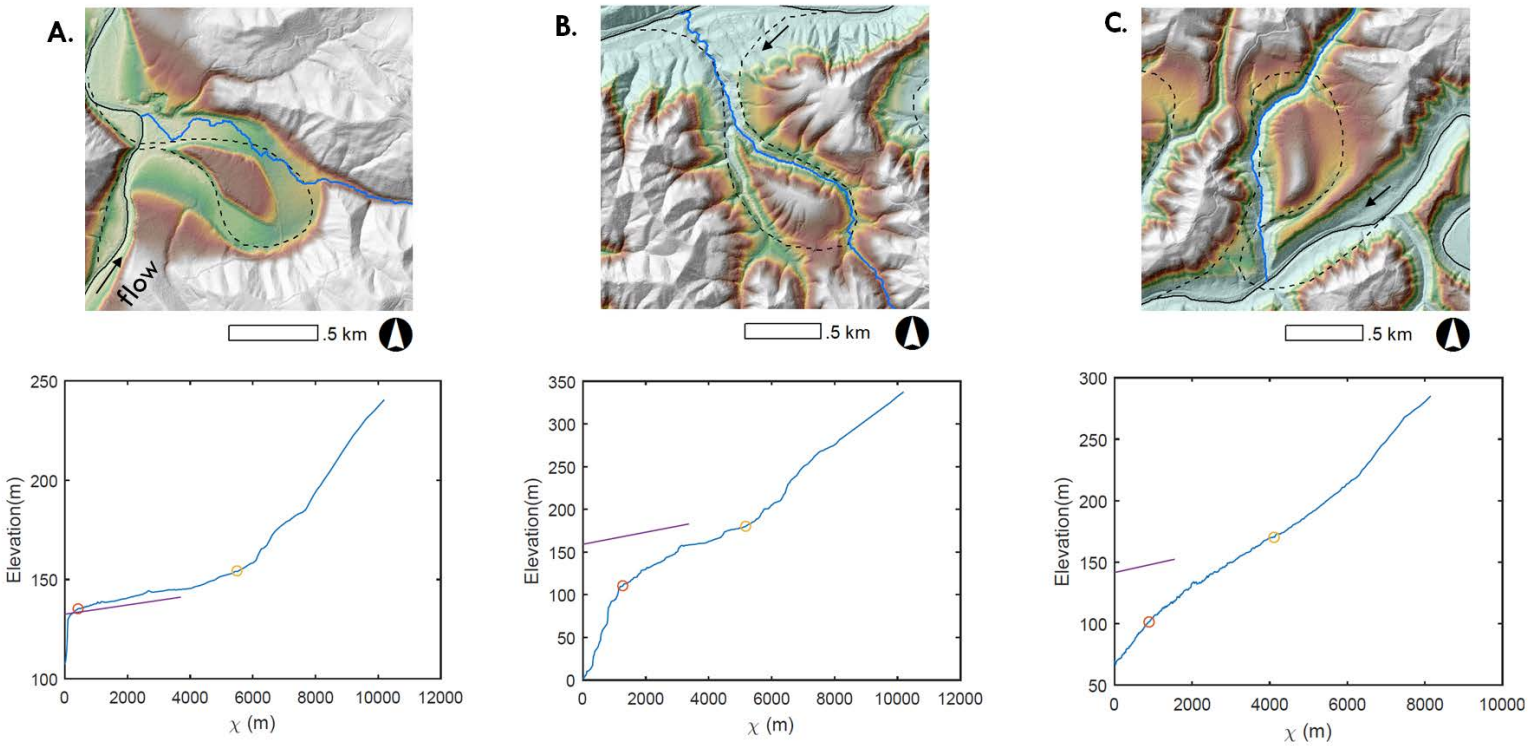

Figure 3. Tributaries abandoned on cutoff terraces are shown in map and profile view. Colors in the map show relative elevation highlighting the terrace surface, dashed black lines are the inferred pre-cutoff thalweg, black is the modern main stem, and blue is the tributary path. In the χ profiles, blue lines are the tributary profiles, purple lines are the inferred original main stem terrace profiles, and the red and yellow dots bracket the profile convexity. Example A has not incised much into the terrace surface despite significant mainstem incision; a depositional fan can be seen at the site of the old confluence, C has progressed farthest towards a new steady state, and B is an intermediate example.

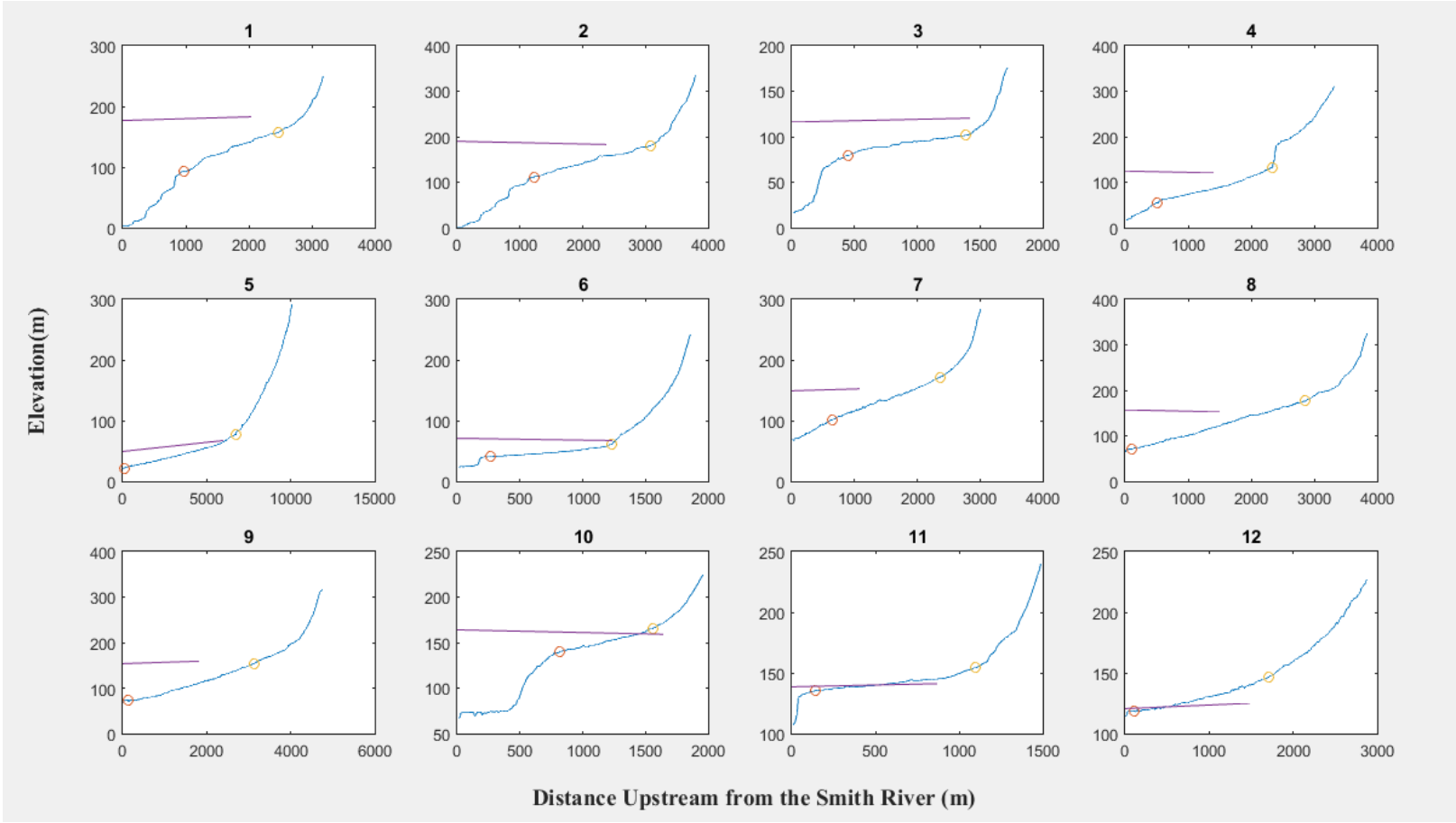

Figure 4. Longitudinal profiles of tributaries crossing neck cutoff terraces. Purple lines are the inferred initial terrace surfaces, red and yellow dots bracket the profile convexities. See fig. 1 for reference map.

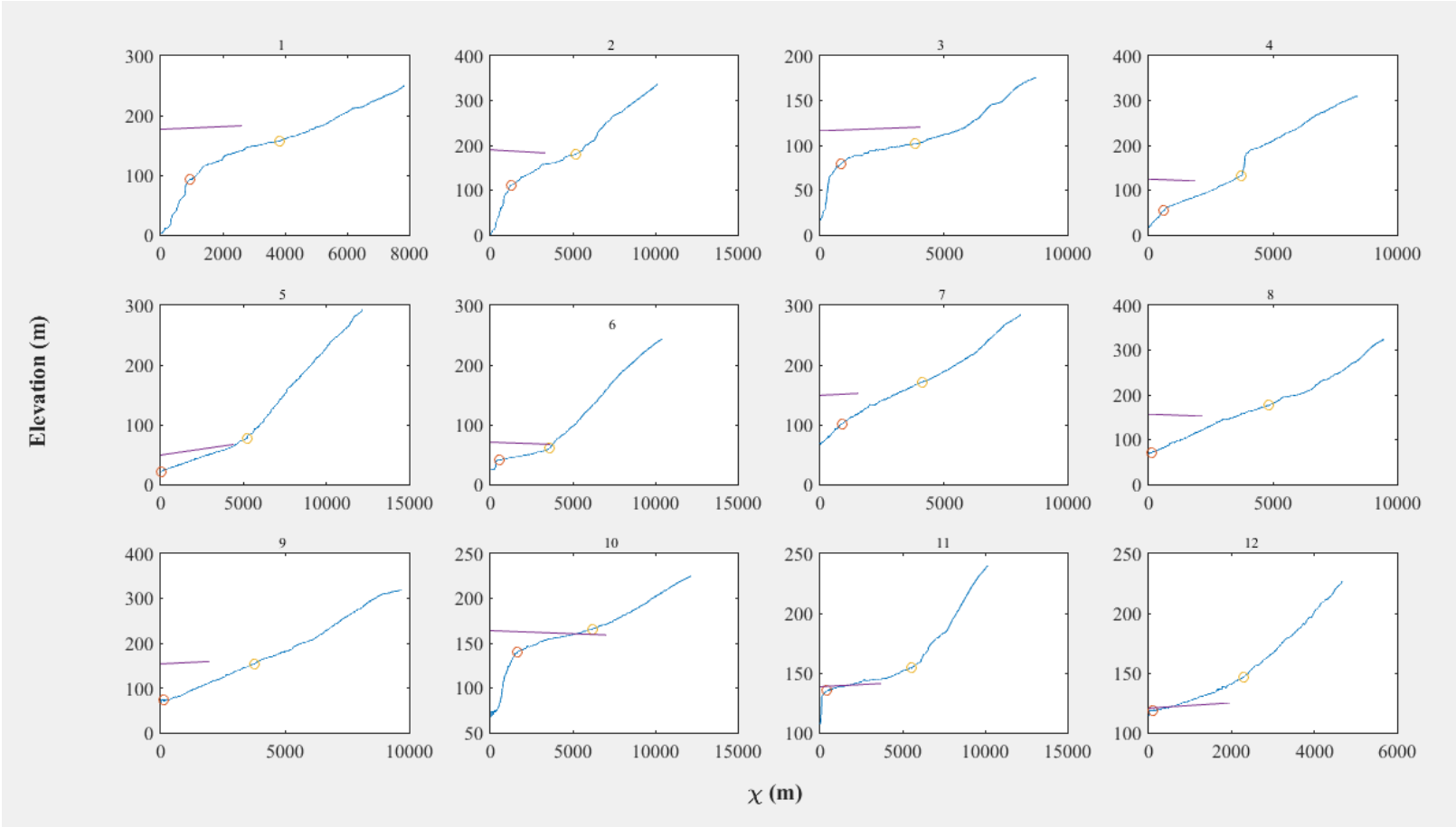

Figure 5. χ profiles of tributaries crossing neck cutoff terraces. Purple lines are the inferred initial terrace surfaces, red and yellow dots bracket the profile convexities. See fig. 1 for reference map.

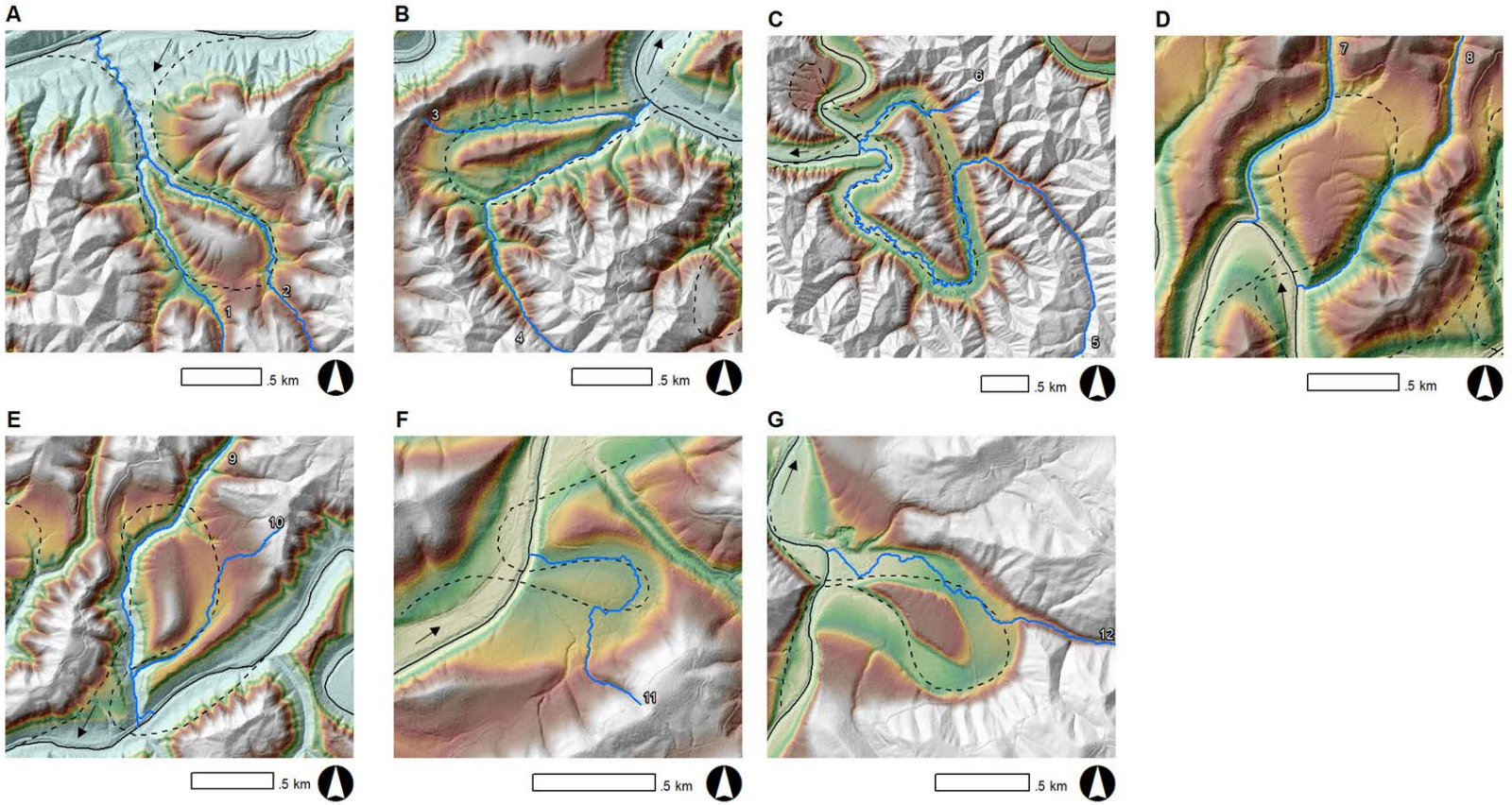

Figure 6. Neck cutoff terraces. Solid black line is the main stem, dashed is pre-cutoff main stem, blue are tributaries. See fig. 1 for reference map.

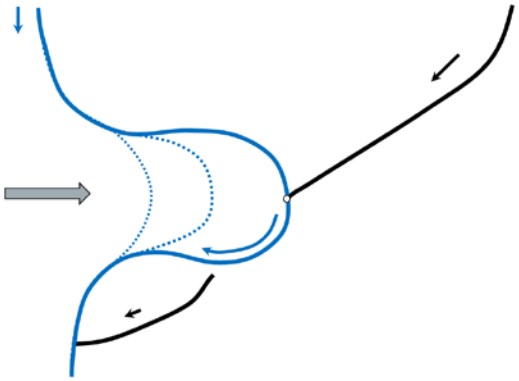

Figure 7. Capture by propagating meander bend.

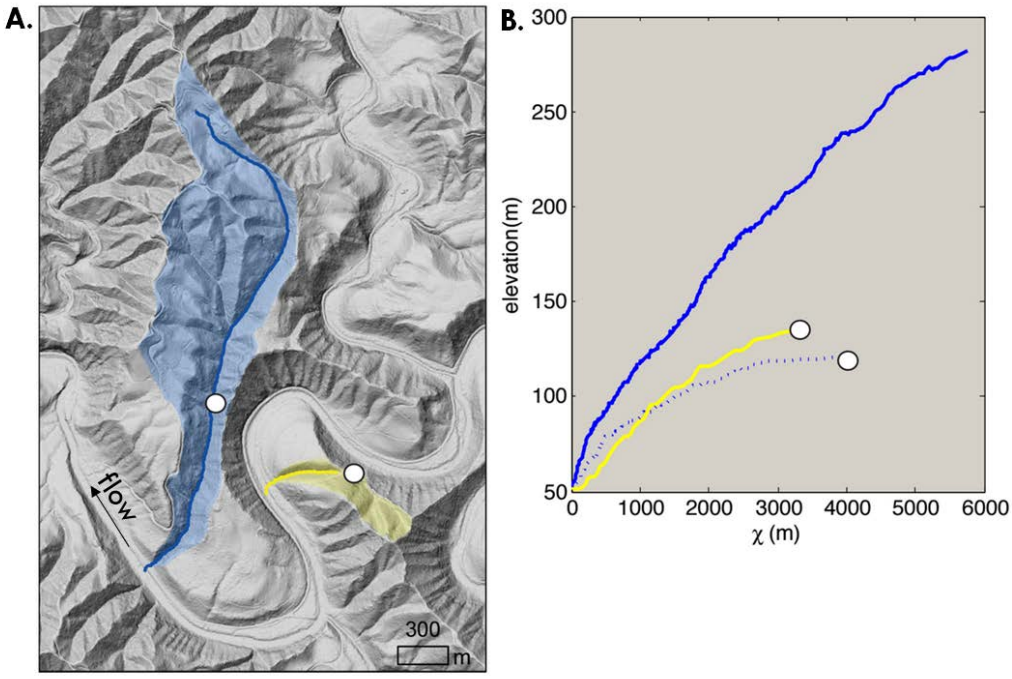

Figure 8. a. Blue tributary and watershed are in imminent danger of capture from the propagating main stem channel. Upon capture, the upper portion of the tributary (above white dot) will join the main stem at the capture point at the leading edge of the meander bend. The lower portion will lose the majority of its catchment area. The yellow tributary has already lost its upper watershed to capture. **b.** χ profiles of these tributaries. The blue tributary is quite straight indicating it is well adjusted to steady state. The blue dashed and yellow lines show the post-capture lower reach. These fall well below the steady state line indicating they have less erosive potential than before.

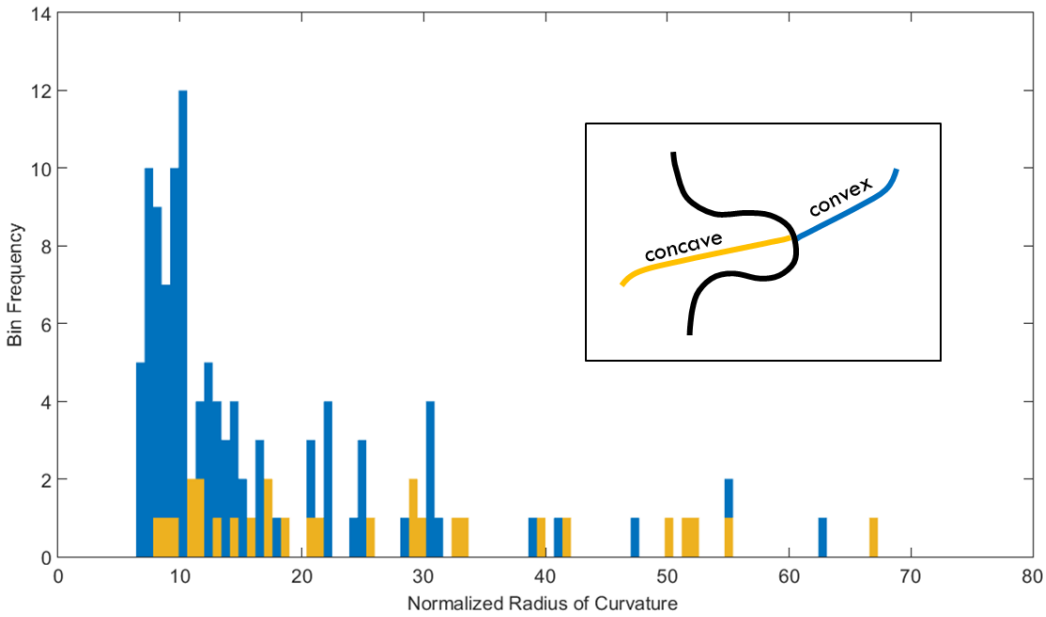

Figure 9. Sinuosity of the main stem Smith River at each tributary junction. Tributaries in dark grey are joining from the inside of the bend and light colored are joining from the outside. Hence the spike in frequency at tight curvatures represents tributaries that join at the leading edge of propagating meander bends.

Cutoff Terrace	main stem incision below terrace (m)	estimated time since cutoff (yr)	tributary	projected incision to equilibrium χ profile (m)	time until relief is available to equilibrate (yr)	incision past equilibrium projection (m)	transience time beyond projection (yr)
A	181	1.8E+06 - 5.4E+06	1	116	1.2E+06 - 3.5E+06	65	6.5E+05 - 2.0E+06
			2	183	1.8E+06 - 5.5E+06	n/a	n/a
B	105	1.0E+06 - 3.1E+06	3	85	8.5E+05 - 2.6E+06	19	1.9E+05 - 5.8E+05
			4	69	6.9E+05 - 2.1E+06	35	3.5E+05 - 1.1E+06
C	47	4.7E+05 - 1.4E+06	5	153	1.5E+06 - 4.6E+06	n/a	n/a
			6	107	1.1E+06 - 3.2E+06	n/a	n/a
D	89	8.9E+05 - 2.7E+06	7	106	1.1E+06 - 3.2E+06	n/a	n/a
			8	128	1.3E+06 - 3.8E+06	n/a	n/a
E	92	9.2E+05 - 2.8E+06	9	121	1.2E+06 - 3.6E+06	n/a	n/a
			10	60	6.0E+05 - 1.8E+06	32	3.2E+05 - 9.6E+05
F	34	3.4E+05 - 1.0E+06	11	95	9.5E+05 - 2.9E+06	n/a	n/a
G	9	9.1E+04 - 2.7E+05	12	56	5.6E+05 - 1.7E+06	n/a	n/a
average		7.9E+05 - 2.4E+06			1.1E+06 - 3.2E+06		3.8E+05 - 1.1E+06

Table 1. Timescales of transience estimated from terrace and tributary topography. It has been an average 10^6 years since these main stem cutoffs occurred, and hence since transience begun on adjoining tributaries. The minimum time to re-equilibration for these tributaries (in terms of necessary main stem relief) is on average 1-3ma, but some profiles continue to exhibit large convexities over 10^5 years past this minimum estimate.

Thesis Conclusion:

In this thesis I have developed a process-based, and generalizable foundation for understanding and investigating actively meandering bedrock rivers. I argue that lateral erosion into bedrock cut banks is possible only where weathering makes bedrock susceptible to fluid erosion, and where colluvium from the retreating bank cannot accumulate and armor the bank from further erosion. In Pescadero Creek, mudstone bedrock disintegrates (slakes) anywhere it is scoured clean and subjected to drying at the surface. Deviations in fluid shear stress caused by the curvature of a meander bend are strong enough to keep cut bank bedrock bare, and point bar bedrock protected by bars that grade upslope into soil. Therefore the same flow patterns recognized to drive meandering in alluvial rivers can dictate the spatial pattern of erosion in bedrock as well. These requirements for bedrock meandering can be generalized for any river, and we show that in channels in basalt in a tropical climate, chemical weathering fulfills the same role as physical weathering did in the mudstone. By making the connection between the process requirements of meandering and climate-dependent weathering processes, we show one way bedrock channel sinuosity can reflect a river's formative climate patterns.

Investigations of sinuous bedrock rivers have enticed geomorphologist to wonder about formative processes for over 100 years, but without a process-based understanding of these beautiful landforms, it was difficult to test hypotheses. Climate, tectonics, rock mechanics and mineralogy come interact in bedrock rivers to make up the scaffolding of landscapes. With such interesting internal dynamics,

actively meandering bedrock rivers not only hold information about their geomorphic past, but can teach us a lot about fundamental geomorphic processes. For example, the autogenic transience they add to drainage networks changes patterns of erosion and routing of sediment that are important to understand both on human timescales for predicting sediment storage and salmonid habitat, and on glacial timescales to understand strath terrace formation, knick points and channel convexities.

Bibliography:

Barbour, J. R., 2008, The origin and significance of sinuosity along incising bedrock rivers.

Chadwick, O. A., Gavenda, R. T., Kelly, E. F., Ziegler, K., Olson, C. G., Elliott, W. C., and Hendricks, D. M., 2003, The impact of climate on the biogeochemical functioning of volcanic soils: Chemical Geology, v. 202, no. 3, p. 195-223.

Davis, W. M., 1893, The Topographic Maps of the United States Geological Survey: Science, v. 21, no. 534, p. 225-227.

Dietrich, W. E., Smith, J. D., and Dunne, T., 1979, Flow and sediment transport in a sand bedded meander: The Journal of Geology, p. 305-315.

Dury, G. H., 1965, Theoretical implications of underfit streams, US Government Printing Office.

Dury, G. H., 1972, Incised meanders: inheritance, statistical testing, and the GIGO principle: Area, p. 281-284.

Einstein, A., 1926, The Cause of the Formation of Meanders in the Courses of Rivers and of the So-Called Baer's Law: Die Naturwissenschaften, v. 14, p. 653-684.

Finnegan, N. J., and Dietrich, W. E., 2011, Episodic bedrock strath terrace formation due to meander migration and cutoff: Geology, v. 39, no. 2, p. 143-146.

Giambelluca, T. W., Chen, Q., Frazier, A. G., Price, J. P., Chen, Y.-L., Chu, P.-S., Eischeid, J. K., and Delparte, D. M., 2013, Online rainfall atlas of Hawai'i: Bulletin of the American Meteorological Society, v. 94, no. 3, p. 313-316.

Goodfellow, B. W., Chadwick, O. A., and Hilley, G. E., 2014, Depth and character of rock weathering across a basaltic-hosted climosequence on Hawai 'i: Earth Surface Processes and Landforms, v. 39, no. 3, p. 381-398.

Han, J. W., Gasparini, N. M., Johnson, J. P. L., and Murphy, B. P., 2014, Modeling the influence of rainfall gradients on discharge, bedrock erodibility, and river profile evolution, with application to the Big Island, Hawai'i: Journal of Geophysical Research-Earth Surface, v. 119, no. 6, p. 1418-1440.

Hancock, G. S., Small, E. E., and Wobus, C., 2011, Modeling the effects of weathering on bedrock-floored channel geometry: Journal of Geophysical Research-Earth Surface, v. 116.

Hasbargen, L. E., and Paola, C., 2000, Landscape instability in an experimental drainage basin: Geology, v. 28, no. 12, p. 1067-1070.

Heimsath, A. M., Dietrich, W. E., Nishiizumi, K., and Finkel, R. C., 2001, Stochastic processes of soil production and transport: Erosion rates, topographic variation and cosmogenic nuclides in the Oregon Coast Range: Earth Surface Processes and Landforms, v. 26, no. 5, p. 531-552.

Hotchkiss, S., Vitousek, P. M., Chadwick, O. A., and Price, J., 2000, Climate cycles, geomorphological change, and the interpretation of soil and ecosystem development: Ecosystems, v. 3, no. 6, p. 522-533.

Howard, A. D., 1992, Modeling channel migration and floodplain sedimentation in meandering streams: Lowland floodplain rivers: geomorphological perspectives, p. 1-41.

Howard, A. D., Dietrich, W. E., and Seidl, M. A., 1994, Modeling fluvial erosion on regional to continental scales: Journal of Geophysical Research-Earth Surface, v. 99, no. B7, p. 13-13.

Howard, A. D., and Kerby, G., 1983, Channel changes in badlands: Geological Society of America Bulletin, v. 94, no. 6, p. 739-752.

Ikeda, S., Parker, G., and Sawai, K., 1981, Bend theory of river meanders. Part 1. Linear development: Journal of Fluid Mechanics, v. 112, p. 363-377.

Johnson, K. N., and Finnegan, N. J., 2015, A lithologic control on active meandering in bedrock channels: Geological Society of America Bulletin, v. 127, no. 11-12, p. 1766-1776.

Kobor, J. S., and Roering, J. J., 2004, Systematic variation of bedrock channel gradients in the central Oregon Coast Range: implications for rock uplift and shallow landsliding: Geomorphology, v. 62, no. 3-4, p. 239-256.

Lanphere, M. A., and Frey, F. A., 1987, Geochemical evolution of Kohala volcano, Hawaii: Contributions to Mineralogy and Petrology, v. 95, no. 1, p. 100-113.

Lavé, J., and Avouac, J. P., 2000, Active folding of fluvial terraces across the Siwaliks Hills, Himalayas of central Nepal: Journal of Geophysical Research: Solid Earth (1978--2012), v. 105, no. B3, p. 5735-5770.

Leopold, L. B., and Bull, W. B., 1979, Base level, aggradation, and grade: Proceedings of the American Philosophical Society, p. 168-202.

Leopold, L. B., and Wolman, M. G., 1960, River Meanders: Geological Society of America Bulletin, v. 71, no. 6, p. 769.

McDougall, I., and Swanson, D. A., 1972, Potassium-argon ages of lavas from the Hawi and Pololu volcanic series, Kohala volcano, Hawaii: Geological Society of America Bulletin, v. 83, no. 12, p. 3731-3738.

Menking, J. A., Han, J., Gasparini, N. M., and Johnson, J. P., 2013, The effects of precipitation gradients on river profile evolution on the Big Island of Hawai'i: Geological Society of America Bulletin, v. 125, no. 3-4, p. 594-608.

Montgomery, D. R., 2004, Observations on the role of lithology in strath terrace formation and bedrock channel width: American Journal of Science, v. 304, no. 5, p. 454-476.

Moon, V., and Jayawardane, J., 2004, Geomechanical and geochemical changes during early stages of weathering of Karamu Basalt, New Zealand: Engineering geology, v. 74, no. 1, p. 57-72.

Murphy, B. J., JPL; Gasparini, NM;, Sklar, LS, in press, Chemical weathering as a mechanism for the climatic control of bedrock river incision: Nature.

Perron, J. T., and Royden, L., 2013, An integral approach to bedrock river profile analysis: Earth Surface Processes and Landforms, v. 38, no. 6, p. 570-576.

Personius, S. F., 1995, Late Quaternary stream incision and uplift in the forearc of the Cascadia subduction zone, western Oregon: Journal of Geophysical Research, v. 100, p. 20,193-120,210.

Personius, S. F., Kelsey, H. M., and Grabau, P. C., 1993, Evidence for regional stream aggradation in the central Oregon Coast Range during the Pleistocene-Holocene transition: Quaternary Research, v. 40, no. 3, p. 297-308.

Porder, S., Hilley, G. E., and Chadwick, O. A., 2007, Chemical weathering, mass loss, and dust inputs across a climate by time matrix in the Hawaiian Islands: Earth and Planetary Science Letters, v. 258, no. 3, p. 414-427.

Reneau, S. L., and Dietrich, W. E., 1991, Erosion Rates in the Southern Oregon Coast Range - Evidence for an Equilibrium between Hillslope Erosion and Sediment Yield: Earth Surface Processes and Landforms, v. 16, no. 4, p. 307-322.

Rich, J. L., 1914, Certain types of stream valleys and their meaning: The Journal of Geology, v. 22, no. 5, p. 469-497.

Sanderson, M., 1993, Prevailing trade winds: climate and weather in Hawaii, University of Hawaii Press.

Schoenbohm, L., Whipple, K., Burchfiel, B., and Chen, L., 2004, Geomorphic constraints on surface uplift, exhumation, and plateau growth in the Red River region, Yunnan Province, China: Geological Society of America Bulletin, v. 116, no. 7-8, p. 895-909.

Shyu, J. B. H., Sieh, K., Avouac, J.-P., Chen, W.-S., and Chen, Y.-G., 2006, Millennial slip rate of the Longitudinal Valley fault from river terraces: Implications for convergence across the active suture of eastern Taiwan: Journal of Geophysical Research, v. 111, no. B8.

Sklar, L. S., and Dietrich, W. E., 2001, Sediment and rock strength controls on river incision into bedrock: Geology, v. 29, no. 12, p. 1087-1090.

Small, E. E., Blom, T., Hancock, G. S., Hynek, B. M., and Wobus, C. W., 2015, Variability of rock erodibility in bedrock-floored stream channels based on abrasion mill experiments: Journal of Geophysical Research: Earth Surface, v. 120, no. 8, p. 1455-1469.

Snyder, N. P., Whipple, K. X., Tucker, G. E., and Merritts, D. J., 2000, Landscape response to tectonic forcing: Digital elevation model analysis of stream profiles in the Mendocino triple junction region, northern California: Geological Society of America Bulletin, v. 112, no. 8, p. 1250-1263.

Spengler, S. R., and Garcia, M. O., 1988, Geochemistry of the Hawi lavas, Kohala volcano, Hawaii: Contributions to Mineralogy and Petrology, v. 99, no. 1, p. 90-104.

Stark, C. P., Barbour, J. R., Hayakawa, Y. S., Hattanji, T., Hovius, N., Chen, H., Lin, C. W., Horng, M. J., Xu, K. Q., and Fukahata, Y., 2010, The climatic signature of incised river meanders: Science, v. 327, no. 5972, p. 1497-1497.

Stearns, H. T., and Macdonald, G. A., 1946, Geology and ground-water resources of the island of Hawaii: Honolulu Advertising.

Stock, J., and Dietrich, W. E., 2003, Valley incision by debris flows: Evidence of a topographic signature: Water Resources Research, v. 39, no. 4.

Survey, U. S. G., National Hydrography Data Set, http://nhd.usgs.gov/.

USGS, The National Map, United States Geological Survey http://nationalmap.gov/

USGS, D., Inc. (DG) and NRCS, 2012, High Resolution Ortho County Mosaic (Natual Color), Purpose: The orthophoto mosaics serve a wide variety of purposes including interim mapping, recording land use information, field references for geographic information system and as a tool for revision of digital line graphs and topographic maps.

Whipple, K. X., 2004, Bedrock rivers and the geomorphology of active orogens: Annu. Rev. Earth Planet. Sci., v. 32, p. 151-185.

Willett, S. D., McCoy, S. W., Perron, J. T., Goren, L., and Chen, C. Y., 2014, Dynamic Reorganization of River Basins: Science, v. 343, no. 6175, p. 1117

Winslow, A., 1893, The Osage River and its meanders: Science, v. 22, no. 546, p. 31-32.

Wobus, C., Whipple, K. X., Kirby, E., Snyder, N., Johnson, J., Spyropolou, K., Crosby, B., and Sheehan, D., 2006, Tectonics from topography: Procedures, promise, and pitfalls: Geological Society of America Special Papers, v. 398, p. 55-74.

Wolfe, E., & Morris, J., 1996, Geologic map of the Island of Hawai‘i.

Yang, R., Willett, S. D., and Goren, L., 2015, In situ low-relief landscape formation as a result of river network disruption: Nature, v. 520, no. 7548, p. 526-529.